Anion induced and inhibited circumrotation of a [2]catenane†

Ka-Yuen Ng,[a] Vitor Felix,[b] Sérgio M. Santos,[b] Nicholas H. Rees[a] and Paul D. Beer*[a]

Received (in Austin, TX, USA) 16th December 2007, Accepted 9th January 2008
First published as an Advance Article on the web 30th January 2008
DOI: 10.1039/b719304a

The first example of a catenane capable of performing circumrotation *via* an anion switching methodology is described; of particular interest is a conformational locking mechanism which results from chloride coordination in the catenane binding cavity.

Inspired by the potential applications mechanically bonded molecules may have as molecular switches and machines, the interest being shown in their construction and surface assembly is ever increasing.[1] However, the use of rotaxane and catenane cavities as binding domains for the recognition and sensing of guest species remains largely underdeveloped[2] which is surprising given their unique three-dimensional topological interlocked cavity design. In addition, such mechanically bonded 'host' molecules have the possibility of exhibiting host–guest binding induced molecular-machine like behaviour.[3] Whereas cations have been frequently used to effect switching between states,[4] by contrast examples of anion mediated interlocked switches are rare and have been, to our knowledge, restricted to rotaxane based systems.[5] We report herein a new [2]catenane ($\mathbf{1}^+$) which undergoes phenolate anion induced intra-ring circumrotation of one macrocycle around the other on addition of base. Furthermore, chloride anion recognition at the catenane's binding site inhibits the rotation process.

Adapting our recently reported general method of using anions to template the formation of a range of interpenetrated and interlocked structures,[6] the new [2]catenane $\mathbf{1}^+Cl^-$ was synthesised in 37% yield by mixing equimolar amounts of pyridinium containing macrocycle $\mathbf{2}^+I^-$ and acyclic bis-vinyl derivative **3** in the presence of TBA chloride template, followed by addition of Grubbs' first generation RCM catalyst (Scheme 1). Purification by column chromatography and subsequent anion exchange afforded the target catenane $\mathbf{1}^+PF_6^-$ which was characterised by ^1H, ^{13}C, ^{19}F NMR and electrospray MS (see ESI†).

ROESY ^1H–^1H NMR spectroscopy was used to determine the relative co-conformational orientations of the two macrocyclic rings of $\mathbf{1}^+PF_6^-$ in 9 : 1 *d*-chloroform : d_6-DMSO solution. Of particular interest were the observed through space proton–proton correlation signals between the *ortho*-pyridinium proton *b* of the pyridinium macrocycle with the hydroquinone and polyether protons of the phenolic containing macrocycle (see dotted lines in Fig. S7†). This is indicative of the expected intercalation of the electron deficient positively charged pyridinium ring motif between the electron rich hydroquinone groups stabilised by favourable π–π stacking interactions (Fig. 1).

The addition of one molar equiv. of base DBU or phosphazene base P_1-^{t}Bu-tris(tetramethylene)[7] to $\mathbf{1}^+PF_6^-$ resulted in significant downfield shifts of the pyridinium *para* proton *c* and amide proton *d* in a variety of solvents including 9 : 1 *d*-chloroform : d_6-DMSO (H_c $\Delta\delta$ = 0.49 ppm, H_d $\Delta\delta$ = 0.40 ppm), d_3-acetonitrile (H_c $\Delta\delta$ = 0.93 ppm, H_d $\Delta\delta$ = 1.70 ppm), d_3-nitromethane (H_c $\Delta\delta$ = 0.15 ppm, H_d $\Delta\delta$ = 0.27 ppm)[8] and d_6-DMSO (H_c $\Delta\delta$ = 0.09 ppm, H_d $\Delta\delta$ = 0.10 ppm) (Fig. 2). Similar observations were also noted when N^1,N^3-bishexyl-5-hydroxyisophthalamide was added to the pyridinium macrocycle $\mathbf{2}^+PF_6^-$ in the presence of base. These results suggest that following deprotonation of the catenane's phenol group by base, the presence of the phenolate anion in the isophthalamide containing macrocycle induces the pyridinium macrocycle to undergo a circumrotation which results in the negatively charged phenolate anion being stabilised *via* hydrogen bonding with the bis-amide pyridinium motif's cleft (Scheme 2). Further evidence for the phenolate anion induced circumrotation of the catenane comes from the absence of any pyridinium proton *b*–hydroquinone and polyether proton correlation signals in the rotated conformer's ROESY spectrum (see ESI†).

It is noteworthy that the addition of trifluoroacetic acid (TFA) reverses the rotation process back to the catenane's intercalated pyridinium group co-conformation.

It was of further interest to investigate whether chloride anion complexation in the unique catenane's interlocked binding pocket would inhibit the phenolate anion induced

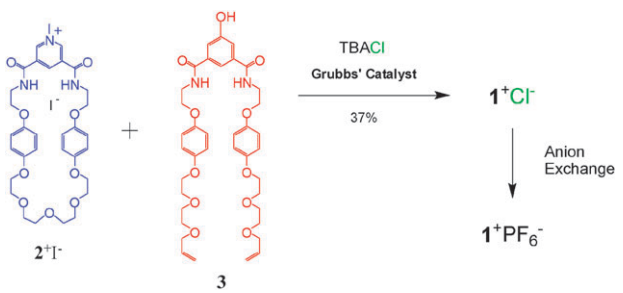

Scheme 1 Synthesis of [2]catenane $\mathbf{1}^+PF_6^-$.

[a] *Inorganic Chemistry Laboratory, Department of Chemistry, University of Oxford, South Parks Road, Oxford, UK OX1 3QR. E-mail: paul.beer@chem.ox.ac.uk; Fax: +44 (0)1865-272690; Tel: +44 (0)1865-285142*
[b] *Departamento de Química, CICECO e Escola Superior de Saúde, Universidade de Aveiro, 3810-193 Aveiro, Portugal. E-mail: vitor.felix@ua.pt; Fax: +351 234-370084; Tel: +351 234-370729*

† Electronic supplementary information (ESI) available: Synthesis and characterisation data for compounds **1–3**, general procedures for ^1H NMR titrations and ROESY spectra and supporting molecular mechanics structures. See DOI: 10.1039/b719304a

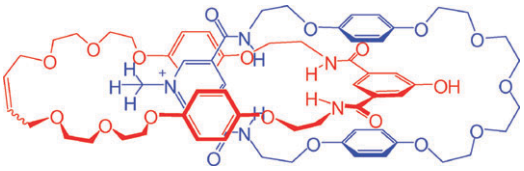

Fig. 1 Structure of catenane $\mathbf{1}^+$.

rotation process. Proton NMR titration experiments of $\mathbf{1}^+PF_6^-$ with TBA chloride in 9 : 1 *d*-chloroform : d_6-DMSO revealed typical downfield shifts of both types of amide protons, *d* and *g*, along with pyridinum/aromatic *c* and *f* protons indicative of halide encapsulation. Subsequent addition of phosphazene base P_1, however, did not result in any significant change in the spectrum (Fig. 3).

The ROESY spectrum of $\mathbf{1}^+Cl^-$ was recorded before and after the addition of base. Both ROESY spectra show that all the important correlation peaks are preserved after deprotonation (see ESI†). This suggests chloride ion complexation in the catenane binding pocket inhibits the pyridinium containing macrocycle from rotating to the phenolate site on base addition.

Further insights into the catenane co-conformations of $\mathbf{1}^+$, **4** and $\mathbf{4}\cdot Cl^-$ were obtained by molecular dynamics (MD) simulations, using the AMBER9[9] software. The lowest energy conformers for these three interlocked structures were obtained in the gas phase by simulated annealing methods. Subsequently, their dynamic behaviour in solution was evaluated in acetonitrile at 300 K during 10 ns, using unconstrained molecular dynamics simulations.† The molecular mechanics (MM) lowest energy structure found for $\mathbf{1}^+$ (Fig. 4) exhibits the pyridinium and phenol moieties intercalated between the two hydroquinone aromatic rings of the ether linkages of the opposite chains, at average interplanar distances consistent with the existence of π–π stacking interactions. The OH group of the phenolic ring is hydrogen bonded to the central ether oxygen of the pyridinium macrocycle at an O–H···O distance of 1.81 Å. It is noteworthy that the amide groups of the pyridinium unit adopt a *syn* disposition while those from the phenol bisamide cleft are *anti*. This co-conformation is stabilised by two N–H···O hydrogen bonds between an amide carbonyl of the phenolic chain and the two N–H binding sites of the pyridinium macrocycle, at N–H···O distances of 2.35 and 2.23 Å.

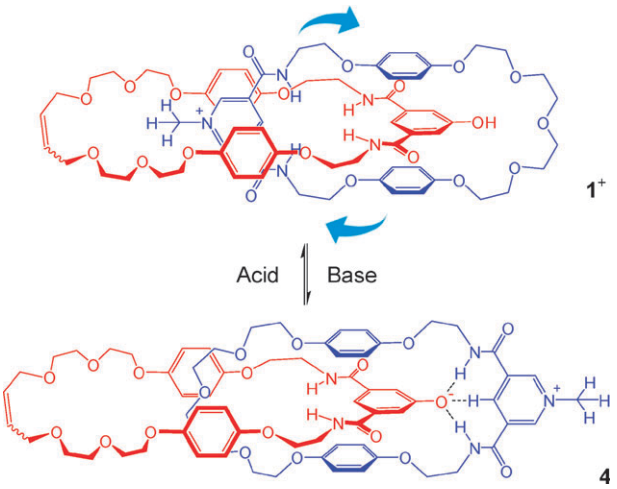

Scheme 2 Strategy for anion induced circumrotation.

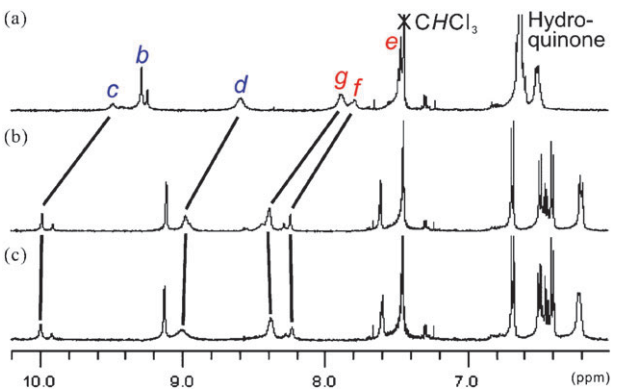

Fig. 3 ^{1}H NMR titration (500 MHz, 298 K, 9 : 1 *d*-chloroform : d_6-DMSO) of (a) $\mathbf{1}^+PF_6^-$, (b) addition of 1 molar equiv. of TBACl to (a) and (c) addition of 1 molar equiv. of phosphazene base P_1 to (b).

MD simulations in acetonitrile show that the two $N–H\cdots O_{amide}$ hydrogen bonds occur simultaneously for large periods, at average distances of 2.57(33)[10] and 2.40(32) Å; the binding interactions between the phenol group and the polyether oxygen atoms of the pyridinium macrocycle oscillate between one and two bifurcated $O–H\cdots O_{ether}$ hydrogen bonds.

The conformational analysis carried out for the phenolate [2]catenane **4** yielded a folded interlocked structure with both

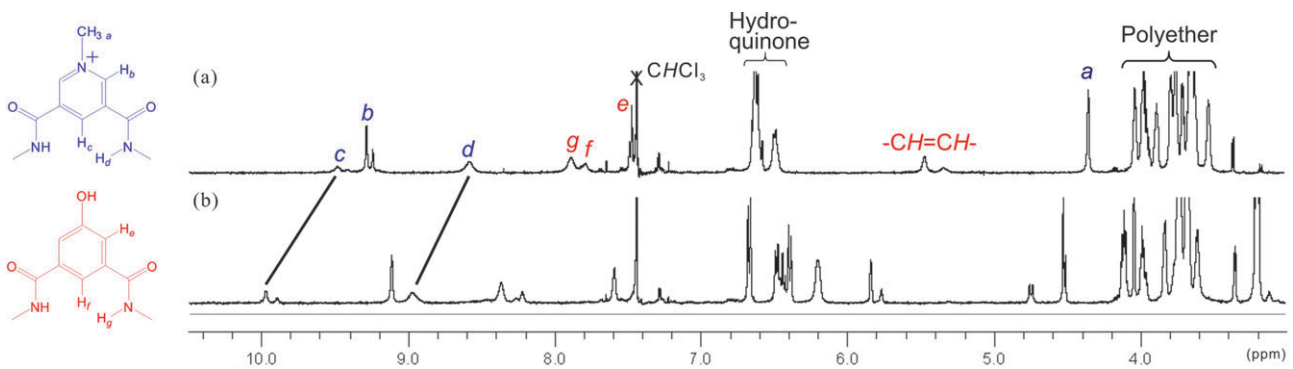

Fig. 2 ^{1}H NMR (500 MHz, 298 K) of (a) $\mathbf{1}^+PF_6^-$ in 9 : 1 *d*-chloroform : d_6-DMSO and (b) after addition of 1 molar equiv. of P_1 base.

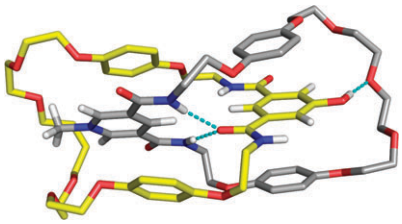

Fig. 4 MM structure of $\mathbf{1}^+$ showing the π–π stacking arrangement and hydrogen bonds (cyan dashes). Only the hydrogen atoms of the bisamide clefts are shown for clarity.

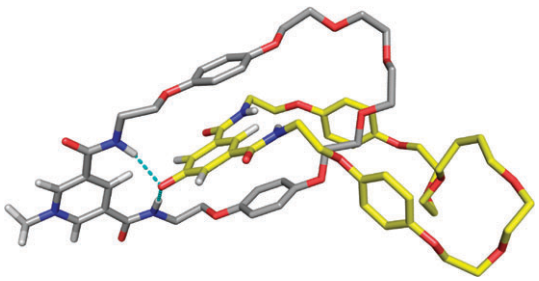

Fig. 5 MM structure of **4** showing the hydrogen bonds between the pyridinium cleft and phenolate oxygen donor. Details as in Fig. 4.

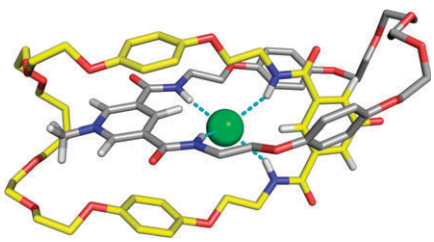

Fig. 6 MM structure of the chloride locked complex $\mathbf{4}\cdot Cl^-$. Details as in Fig. 4.

bisamide groups adopting a *syn* disposition (Fig. S11 in ESI†). However, when this conformation was immersed in acetonitrile and submitted to an MD run, the structure unfolded itself in the first 100 ps, after breaking two N–H···O_{ether} hydrogen bonds, and remained so until the end of the simulation (10 ns). The corresponding molecular mechanics minimised average structure is depicted in Fig. 5. During the course of the simulation, the phenolate ring is maintained intercalated between the two hydroquinone motifs, at interplanar distances consistent with either face-to-face or face-to-edge π–π stacking interactions, whereas the two N–H···$O_{phenolate}$ hydrogen bonds were kept at average distances of 2.23(27) and 2.27(28) Å.

The lowest energy conformation search of $\mathbf{4}\cdot Cl^-$ yielded a structure (Fig. 6) having the chloride encapsulated into the [2]catenane cavity in a tetrahedral fashion, establishing four N–H···Cl^- hydrogen bonds ranging from 2.26 to 2.50 Å. The corresponding MD simulation shows that the four hydrogen bonds occur simultaneously during most of the simulation period leading to N-H···Cl average distances of 2.46(18), 2.46(18), 2.60(22) and 2.59(22) Å.

The MD structures thus described for $\mathbf{1}^+$, **4** and $\mathbf{4}\cdot Cl^-$ are entirely consistent with ^{1}H NMR solution studies.

The design of anion switchable interlocked systems is continuing in our laboratories.

Ka-Yuen Ng would like to thank the Clarendon Fund and the Overseas Research Student (ORS) Awards Scheme for a scholarship. Sérgio M. Santos acknowledges Fundação para a Ciência e Tecnologia (FCT) for financial support in the form of PhD scholarship SFRH/BD/29596/2006.

Notes and references

1 (*a*) V. Serreli, C. F. Lee, E. R. Kay and D. A. Leigh, *Nature*, 2007, **445**, 523; (*b*) F. Arico, J. D. Badjic, S. J. Cantrill, A. H. Flood, K. C. F. Leung, Y. Liu and J. F. Stoddart, *Top. Curr. Chem.*, 2005, **249**, 203; (*c*) J.-P. Sauvage and C. Dietrich-Buchecker, *Molecular Catenanes, Rotaxanes and Knots*, Wiley-VCH, Chichester, 1999.

2 For some examples see: (*a*) S. R. Bayly, T. M. Gray, M. J. Chmielewski, J. J. Davis and P. D. Beer, *Chem. Commun.*, 2007, 2234; (*b*) N. Kameta, Y. Nagawa, M. Karikomi and K. Hiratani, *Chem. Commun.*, 2006, 3714; (*c*) D. Curiel and P. D. Beer, *Chem. Commun.*, 2005, 1909; (*d*) I. Smukste, B. E. House and D. B. Smithrud, *J. Org. Chem.*, 2003, **68**, 2559; (*e*) M. J. Deetz, R. Shukla and B. D. Smith, *Tetrahedron*, 2002, **58**, 799; (*f*) A. Andrievsky, F. Ahuis, J. L. Sessler, F. Vogtle, D. Gudat and M. Moini, *J. Am. Chem. Soc.*, 1998, **120**, 9712.

3 (*a*) E. R. Kay, D. A. Leigh and F. Zerbetto, *Angew. Chem., Int. Ed.*, 2007, **46**, 72; (*b*) V. Balzani, A. Credi and M. Venturi, *Molecular Devices and Machines: a journey into the nanoworld*, Wiley-VCH, Cambridge, 2003; (*c*) V. Balzani, A. Credi and M. Venturi, *Acc. Chem. Res.*, 2001, **34**(special issue on molecular machines), 409.

4 (*a*) S. J. Loeb, J. Tiburcio and S. J. Vella, *Chem. Commun.*, 2006, 1598; (*b*) J. D. Badjic, C. M. Ronconi, J. F. Stoddart, V. Balzani, S. Silvi and A. Credi, *J. Am. Chem. Soc.*, 2006, **128**, 1489; (*c*) D. A. Leigh, P. J. Lusby, A. M. Z. Slawin and D. B. Walker, *Chem. Commun.*, 2005, 4919; (*d*) U. Letinois-Halbes, D. Hanss, J. M. Beierle, J. P. Collin and J. P. Sauvage, *Org. Lett.*, 2005, **7**, 5753; (*e*) H. R. Tseng, S. A. Vignon and J. F. Stoddart, *Angew. Chem., Int. Ed.*, 2003, **42**, 1491; (*f*) D. A. Leigh, J. K. Y. Wong, F. Dehez and F. Zerbetto, *Nature*, 2003, **424**, 174.

5 (*a*) Y.-L. Huang, W.-C. Hung, C.-C. Lai, Y.-H. Liu, S.-M. Peng and S.-H. Chiu, *Angew. Chem., Int. Ed.*, 2007, **46**, 6629; (*b*) C. F. Lin, C. C. Lai, Y. H. Liu, S. M. Peng and S. H. Chiu, *Chem.–Eur. J.*, 2007, **13**, 4350; (*c*) C. M. Keaveney and D. A. Leigh, *Angew. Chem., Int. Ed.*, 2004, **43**, 1222; (*d*) B. W. Laursen, S. Nygaard, J. O. Jeppesen and J. F. Stoddart, *Org. Lett.*, 2004, **6**, 4167; (*e*) A. M. Brouwer, C. Frochot, F. G. Gatti, D. A. Leigh, L. Mottier, F. Paolucci, S. Roffia and G. W. H. Wurpel, *Science*, 2001, **291**, 2124; (*f*) M. Montalti and L. Prodi, *Chem. Commun.*, 1998, 1461.

6 (*a*) M. D. Lankshear and P. D. Beer, *Acc. Chem. Res.*, 2007, **40**, 657; (*b*) M. D. Lankshear, N. H. Evans, S. R. Bayly and P. D. Beer, *Chem.–Eur. J.*, 2007, **13**, 3861; (*c*) P. D. Beer, M. R. Sambrook and D. Curiel, *Chem. Commun.*, 2006, 2105; (*d*) K.-Y. Ng, A. R. Cowley and P. D. Beer, *Chem. Commun.*, 2006, 3676; (*e*) M. R. Sambrook, P. D. Beer, M. D. Lankshear, R. F. Ludlow and J. A. Wisner, *Org. Biomol. Chem.*, 2006, **4**, 1529; (*f*) M. R. Sambrook, P. D. Beer, J. A. Wisner, R. L. Paul and A. R. Cowley, *J. Am. Chem. Soc.*, 2004, **126**, 15364; (*g*) J. A. Wisner, P. D. Beer, M. G. B. Drew and M. R. Sambrook, *J. Am. Chem. Soc.*, 2002, **124**, 12469.

7 R. Schwesinger, C. Hasenfratz, H. Schlemper, L. Walz, E. M. Peters, K. Peters and H. G. Vonschnering, *Angew. Chem., Int. Ed. Engl.*, 1993, **32**, 1361.

8 Value at 0.6 equiv. of phosphazene base P_1; the peaks broadened into baseline upon further addition of base in d_3-nitromethane.

9 D. A. Case, T. A. Darden, T. E. Cheatham, III, C. L. Simmerling, J. Wang, R. E. Duke, R. Luo, K. M. Merz, D. A. Pearlman, M. Crowley, R. C. Walker, W. Zhang, B. Wang, S. Hayik, A. Roitberg, G. Seabra, K. F. Wong, F. Paesani, X. Wu, S. Brozell, V. Tsui, H. Gohlke, L. Yang, C. Tan, J. Mongan, V. Hornak, G. Cui, P. Beroza, D. H. Mathews, C. Schafmeister, W. S. Ross and P. A. Kollman, *AMBER9*, University of California, San Francisco, 2006.

10 Values in parentheses correspond to the standard deviation of the mean (N = 50 000), so that 2.57(33) is equivalent to 2.57 ± 0.33. The remaining cases will follow this presentation.